

Charged-particle multiplicity distributions in νn and νp charged-current interactions

D. Zieminska,* S. Kunori, C. Y. Chang, G. A. Snow, D. Son, and P. H. Steinberg
University of Maryland, College Park, Maryland 20742

R. A. Burnstein, J. Hanlon, and H. A. Rubin
Illinois Institute of Technology, Chicago, Illinois 60616

R. Engelmann, T. Kafka, and S. Sommars†
State University of New York, Stony Brook, New York 11794

T. Kitagaki, S. Tanaka, H. Yuta, K. Abe, K. Hasegawa, A. Yamaguchi,
K. Tamai, T. Hayashino, Y. Otani, and H. Hayano
Tohoku University, Sendai 980, Japan

C. C. Chang,‡ W. A. Mann, A. Napier, and J. Schneps
Tufts University, Medford, Massachusetts 02155
(Received 28 June 1982)

Charged-hadron multiplicity distributions in νn and νp interactions are measured in an exposure of the Fermilab deuterium-filled 15-foot bubble chamber to a wide-band neutrino beam. Multiplicity moments are studied as functions of the invariant mass of the hadronic system W in the range $1 < W < 15$ GeV. The mean multiplicities for both νn and νp are found to increase logarithmically with W^2 with identical slopes but slightly different intercepts. A linear rise of the dispersion D with the mean multiplicity $\langle n_{\text{ch}} \rangle$ is observed with an approximate slope of 0.35. This value is similar to that found in e^+e^- and $\bar{p}p$ annihilation and is much less than the asymptotic prediction of QCD. A close similarity between D_- vs $\langle n_- \rangle$ in νn and νp interactions is seen. Negative correlations between the multiplicity distributions in the forward and backward hadronic center-of-mass hemispheres are found and discussed.

I. INTRODUCTION

Characteristics of charged-particle multiplicity distributions have been studied extensively in high-energy hadronic collisions and, more recently, in e^+e^- annihilation¹ and in lepton-induced interactions.²⁻⁵ Despite the existence of quantum chromodynamics as a theory of strong interactions, detailed predictions of hadron production are still quite model dependent. It is important to compare lepton-lepton, lepton-hadron, and hadron-hadron interactions in all their manifestations in order to elucidate similarities or differences as well as phenomenological regularities. In this paper we report the first study of charged-hadron multiplicities initiated in high-energy charged-current neutrino interactions on deuteron targets, from which νn and νp collisions from an identical neutrino flux can be separated.

A schematic diagram of a charged-current neutrino interaction is shown in Fig. 1, for the case that

the positive weak-interaction current converts a valence d quark to a u quark, leaving behind a (ud) or (uu) diquark for a neutron or proton target, respectively. In general, we have

$$\nu_\mu + n \rightarrow \mu^- + X^+, \quad X^+ \rightarrow \text{hadrons}, \quad (1a)$$

$$\nu_\mu + p \rightarrow \mu^- + X^{++}, \quad X^{++} \rightarrow \text{hadrons}. \quad (1b)$$

The bubble-chamber technique is well suited for investigation of the multiplicity of charged hadrons, n_{ch} , emitted in each of these reactions.

The behavior of the mean multiplicity $\langle n_{\text{ch}} \rangle$ as a function of energy and the dispersion of these multiplicity distributions are studied and compared with results of other experiments and with theoretical models. The results are discussed in terms of the quark-parton model (QPM), and compared with simple asymptotic predictions of quantum chromodynamics. Multiplicities of charged particles in the forward and backward hemispheres in the hadronic c.m. system, and their correlations, are investigated.

Implications of these results for particle production mechanisms are discussed.

II. EXPERIMENTAL PROCEDURE

The data sample comes from a 328 000-frame exposure of the Fermilab 15-foot deuterium-filled bubble chamber, with a two-plane external muon identifier, to a single-horn focused wide-band neutrino beam produced by 350-GeV/c protons. The sample corresponds to a flux of 4.57×10^{18} protons on target, representing 92% of the exposure. The average neutrino energy is 50 GeV.

The film was scanned twice for events with two or more charged prongs produced by neutral particles. The scanning efficiencies of this double scan are 94% for two-prong events, 98% for three-prong events, and 100% for events with four or more prongs. These events were measured and processed through the TVGP-SQUAW program chain. Events that failed our geometrical reconstruction criteria were remeasured. We accept only those events in the fiducial volume of 16.7 m³ which have $\Delta p/p < 0.5$ for all tracks and which satisfy the charge balance requirement. We further require that the sum of charged-particle longitudinal momenta be greater than 5 GeV/c to reduce background from neutral-hadron-induced events. Two-prong events which are consistent with K^0 or Λ decay or with a γ conversion were removed from the event sample. With these selection criteria, the averaging efficiency varies from 96% to 50% as the multiplicity increases from 2 to ≥ 13 . The overall scanning-measuring efficiency is 84%. The charged-current events are extracted by applying the kinematic method described by Bell *et al.*⁵ We require that p_{TR} , the μ^- transverse momentum relative to the total momentum of other charged particles, be greater than 1 GeV/c.

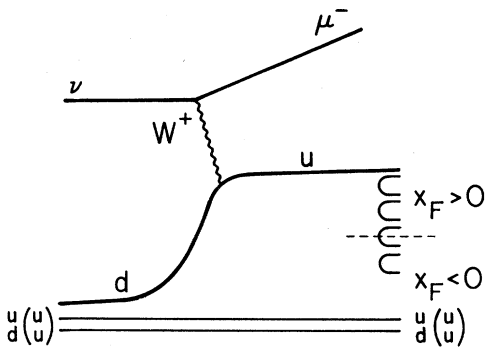


FIG. 1. Schematic diagram of a charged-current $\nu N \rightarrow \mu^- X$ reaction. The valence quark lines correspond to neutron (proton) targets.

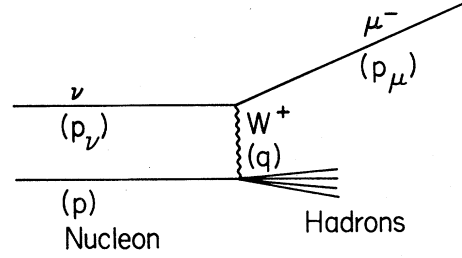


FIG. 2. Kinematic diagram for a charged-current $\nu N \rightarrow \mu^- X$ reaction. Four-momenta are given in parentheses.

A diagram representing a νN interaction is shown in Fig. 2, with our kinematic notation. To correct for missing neutral particles, the neutrino energy is calculated for each event according to the following formula⁶:

$$E_\nu = p_L^\mu + p_L^c \left[1 + \frac{|\vec{p}_T^\mu + \vec{p}_T^c|}{\sum_{i=1}^{n_{ch}} |\vec{p}_{Ti}|} \right], \quad (2)$$

where p_L^μ (p_T^μ) and p_L^c (p_T^c) are, respectively, the longitudinal (transverse) momenta of the μ^- and the charged-hadron system relative to the neutrino direction, and p_{Ti} is the transverse momentum of the i th charged hadron. Only events with $E_\nu > 10$ GeV are accepted for analysis. The effective mass of the hadronic system W is calculated as follows:

$$W^2 = M_p^2 + 2M_p(E_\nu - E_\mu) - Q^2, \quad (3)$$

$$Q^2 = -q^2 = 2E_\nu(E_\mu - p_L^\mu) - m_\mu^2.$$

In Eqs. (3) m_μ and M_p are the muon and proton masses and q^2 is the square of the four-momentum transfer at the leptonic vertex.

A Monte Carlo calculation is used to correct for the number of true charged-current events lost from our sample because of our experimental selection criteria as well as for the small (<6%) number of neutral-current and $\bar{\nu}_\mu$ events included in our sample. Ingredients in this Monte Carlo calculation include the neutrino energy spectrum, obtained from our own data in the bubble chamber, together with theoretical flux calculations, structure functions of the proton and neutron parametrized by Field and Feynman,⁷ hadron distributions based on data from hadronic reactions (longitudinal phase space), and the experimental errors of track measurements in the bubble chamber. The uncorrected (corrected) number of charged-current events in our final νD sample is 11 467 (15 530).

The smearing of W^2 due to the uncertainty in our estimate of the neutrino energy for each event was

TABLE I. Charged-hadron multiplicity distributions for (a) neutrino-neutron charged-current and (b) neutrino-proton charged-current interactions as functions of hadron energy squared W^2 for $E_\nu > 10$ GeV (errors shown are statistical only and do not include systematic errors in the Monte Carlo corrections).

W^2 (GeV ²)	$\langle W^2 \rangle$ (GeV ²)	(a)										Total
		$n_{ch}=1$	3	5	Corrected number of events			9	11	≥ 13		
1-2	1.44	277.6±17.4	1.1±0.3	0	0	0	0	0	0	0	0	278.7
2-3	2.49	292.3±22.4	59.8±6.5	0.1±0.1	0	0	0	0	0	0	0	352.2
3-4	3.50	195.9±18.1	124.3±10.6	0.2±0.1	0	0	0	0	0	0	0	320.4
4-6	4.95	308.2±22.1	356.8±19.7	14.2±3.2	0	0	0	0	0	0	0	679.2
6-8	6.97	235.8±19.3	361.1±20.6	63.4±7.7	1.2±0.8	0	0	0	0	0	0	661.6
8-12	9.92	270.6±20.4	650.6±28.8	237.6±16.6	14.6±3.7	0	0	0	0	0	0	1173.4
12-16	13.92	149.2±14.9	407.8±22.5	312.2±20.3	55.9±7.9	1.8±1.3	0	0	0	0	0	926.9
16-23	19.17	115.8±12.9	499.0±26.7	446.1±26.0	145.5±14.7	12.1±3.8	0	0	0	0	0	1218.5
23-32	27.19	82.6±10.8	354.2±22.7	420.3±25.6	169.7±16.6	34.9±7.4	2.8±2.0	0	0	0	0	1064.5
32-45	37.83	62.3±9.2	238.7±18.6	342.2±23.2	183.4±17.7	68.0±11.0	12.1±4.6	0	0	0	0	906.6
45-63	53.05	38.0±7.1	158.0±14.9	232.2±19.0	175.6±17.3	69.4±11.3	15.0±5.3	0	0	0	0	688.2
63-90	73.96	13.9±4.2	90.2±11.1	138.2±14.3	115.1±13.8	68.9±11.2	15.7±5.6	6.0±3.5	0	0	0	448.0
90-125	105.00	4.9±2.5	41.6±7.4	64.9±9.6	92.6±12.1	33.9±7.8	23.4±6.8	8.8±4.4	0	0	0	270.1
125-225	158.30	10.5±3.5	28.3±5.9	62.3±9.2	72.5±10.5	32.9±7.5	31.7±7.5	10.5±5.3	0	0	0	248.7
Total	28.03	2057.6	3371.0	2334.3	1026.1	321.9	100.7	25.3	0	0	0	9236.9

W^2 (GeV ²)	$\langle W^2 \rangle$ (GeV ²)	(b)										Total
		$n_{ch}=2$	4	6	Corrected number of events			10	12	≥ 14		
1-2	1.58	245.3±15.9	0.2±0.1	0	0	0	0	0	0	0	0	245.5
2-3	2.46	160.3±12.8	19.4±3.7	0	0	0	0	0	0	0	0	179.9
3-4	3.51	151.8±12.2	35.1±5.7	0.2±0.1	0	0	0	0	0	0	0	187.1
4-6	4.98	242.7±16.1	154.0±13.1	5.8±2.1	0.3±0.3	0	0	0	0	0	0	402.8
6-8	6.98	168.4±13.9	198.2±15.4	22.1±4.6	0	0	0	0	0	0	0	388.7
8-12	9.91	242.6±17.4	448.4±24.1	99.4±10.8	8.5±2.8	0	0	0	0	0	0	798.9
12-16	13.89	128.8±13.0	314.0±19.9	168.4±15.1	24.5±5.3	1.0±1.0	0.2±1.0	0	0	0	0	636.9
16-23	19.22	102.0±11.9	372.4±23.3	224.9±18.7	62.9±9.8	5.1±2.6	1.0±1.0	0	0	0	0	768.3
23-32	27.14	69.0±9.8	261.3±19.7	269.3±20.8	84.4±11.9	13.4±4.7	1.5±1.5	0	0	0	0	698.9
32-45	37.85	33.1±4.7	172.4±16.0	203.7±18.1	98.0±13.2	20.5±6.2	3.7±2.6	1.3±1.3	0	0	0	532.7
45-63	52.52	22.1±5.4	117.9±13.0	188.5±17.4	85.5±12.3	43.8±9.1	6.0±3.5	0	0	0	0	463.8
63-90	74.56	7.5±3.1	66.7±9.6	129.9±14.1	87.4±12.2	34.6±8.2	8.4±4.2	4.4±3.1	0	0	0	338.9
90-125	106.80	7.1±2.9	27.7±6.0	90.0±11.4	44.0±8.5	33.7±7.9	10.5±4.7	9.8±4.9	0	0	0	222.8
125-225	161.90	3.4±2.0	31.3±6.3	44.4±7.8	43.7±8.3	27.2±7.0	8.4±4.2	9.2±5.4	0	0	0	167.6
Total	29.41	1584.1	2219.0	1446.6	539.2	179.3	39.7	24.7	0	0	0	6032.6

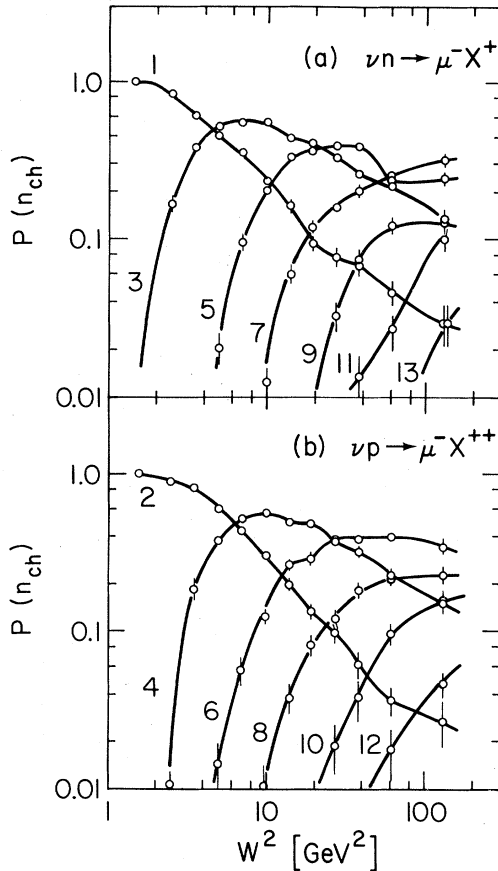


FIG. 3. Normalized topological cross sections versus W^2 for charged-hadron multiplicities. (a) $\nu n \rightarrow \mu^- + (n_{\text{ch}})^+$. (b) $\nu p \rightarrow \mu^- + (n_{\text{ch}})^{++}$. The lines are drawn between experimental points to guide the eye.

also studied by the Monte Carlo method, and the appropriate corrections were applied. The sensitivity of the calculated values of W^2 to the uncertainty of the beam energy determination was examined by using an alternative formula for E_ν in lieu of Eq. (2). In particular, the denominator in the last term was replaced by p_T^c . Only relatively small differences in the final results between these calculations, as indicated below, were observed. The uncertainty in the determination of W due to neutrino energy uncertainty is estimated to be 20% full width at half maximum (FWHM).

Effects arising from close secondary interactions, close V^0 decays and Dalitz pairs were considered. Residual effects of close secondary interactions and V^0 decays were found to be less than 2%. When a single electron or positron was identified this track and another track of opposite charge were removed from the final state if their invariant mass was less than 70 MeV. The effect of unrecognized Dalitz pairs of the multiplicities was estimated to be less

than 1%. No corrections were made for these small effects.

We separate νD events into νn and νp samples, as described by Eqs. 1(a) and 1(b), using the following procedure: events with an even number of prongs plus events with an odd number of prongs that include a visible spectator proton track fall into the νn category; events with an odd number of prongs with no visible spectator track are assigned to the νp category. By spectator we mean an identified proton which is emitted backward in the laboratory frame or forward with a momentum $p < p_0 = 340$ MeV/c. This choice of p_0 gives the expected ratio of the number of backward spectators to the number of forward spectators as calculated from the Moller flux and cross-section ratios.⁸

The νp sample defined in this way contains neutron-target events that have been converted from an even-prong to an odd-prong topology by an interaction of a hadron or a parton in the final state with the proton in the deuteron.⁸ Effects of this rescattering on the results presented here will be discussed later. The νn sample is not contaminated by the rescattering process in deuterium.

III. CHARGED-HADRON MULTIPLICITIES

A. Multiplicity distributions

The multiplicity distributions for charged-current neutrino interactions have been determined for both neutron- and proton-target events. The normalized topological cross sections

$$P(n_{\text{ch}}) = \sigma(n_{\text{ch}}) / \sum_{n_{\text{ch}}} \sigma(n_{\text{ch}})$$

are given in Fig. 3 and the corresponding numbers of events in Table I for 14 W^2 intervals between 1 and 225 GeV^2 . We observe a strong decrease of $P(1)$ and $P(2)$ with energy, indicating the absence of substantial diffractive components. This is a major difference between lepton-nucleon and hadron-nucleon reactions.

B. Average multiplicities

The average charged-particle multiplicities $\langle n_{\text{ch}} \rangle$ for the joint νD sample are given as a function of W^2 in Fig. 4(a). Any visible spectator proton is not included in this prong count. (This choice was made in order to facilitate future A -dependence studies, although it is different from the convention used in hadron-deuteron multiplicity papers.) The average charged-particle multiplicities for νn and νp interactions separately are plotted as functions of W^2 in Fig. 4(b). Above $W^2 = 4 \text{ GeV}^2$ they lie along straight lines parallel to each other with the νp charged multiplicity larger by 0.7. The error bars

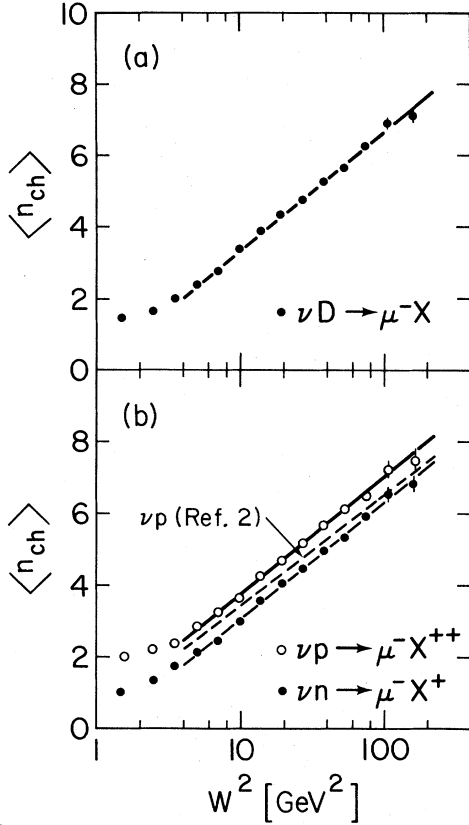


FIG. 4. Average charged-hadron multiplicity $\langle n_{ch} \rangle$ as a function of W^2 . (a) νD events. (b) νn and νp events. The solid lines represent linear fits to the data. The dashed line is the linear fit to the νp data of Ref. 2.

shown do not include the possible systematic uncertainty related to our method of estimating the energy of the incident neutrino. We checked the sensitivity of our results to this uncertainty by applying various methods of calculating W , as explained in Sec. II. The mean multiplicity $\langle n_{ch} \rangle$ at a given W was found to vary within a range of about ± 0.1 units. However, the difference

$$\langle n_{ch} \rangle_{\nu p} - \langle n_{ch} \rangle_{\nu n} \approx 0.70$$

remained unchanged. Above $W = 2$ GeV the mean multiplicities are in very good agreement with a linear dependence on $\ln W^2$, that is,

$$\langle n_{ch} \rangle = A + B \ln W^2. \quad (4)$$

The values of A and B for νD , νn , and νp interactions are given in Table II, along with the results of previous νp experiments.^{2,5}

We confirm that the energy dependence of the mean multiplicity of charged hadrons produced in νN interactions at energies below $W = 15$ GeV is consistent with the scaling hypothesis of the naive quark-parton model.^{7,9} No indication of a more rapid rise of charge multiplicity with W , as has been seen in e^+e^- collisions¹ above 10 GeV, is observed in our data.

A comparison of the mean multiplicities in νn and νp interactions from our experiment with results from νp interactions in hydrogen² allows us to study the difference in the (ud) and (uu) diquark fragmentation and to assess the size of double-scattering effects in deuterium. As seen in Fig. 4(b) the νp data from Ref. 2 lie between the νn and νp data from this experiment.

As mentioned in Sec. II, our νp sample contains events where a primary neutrino interaction on a neutron or a proton is followed by a rescattering inside the deuteron. The differences between the mean multiplicity $\langle n_{ch} \rangle_{\nu p}$ obtained in deuterium and in hydrogen is a measure of the multiplicity of particles produced in the secondary scattering. The values of the observed difference vary between 0.3 and 0.5 and are somewhat larger than the systematic error due to the W^2 scale uncertainty, which is about 0.2. The difference is presumably the result of double-scattering effects, and is quite small.

The difference $\langle n_{ch} \rangle_{\nu p} - \langle n_{ch} \rangle_{\nu n}$, or the corresponding difference between the negative hadron multiplicities $\alpha = \langle n_- \rangle_{\nu n} - \langle n_- \rangle_{\nu p}$, has a simple quark-parton-model interpretation. In the dominant process the d quark which absorbs the intermediate W^+ is transformed into a u quark and is separated from the remaining diquark system (see Fig. 1). The

TABLE II. Parameters of the linear fit to the multiplicity distributions $\langle n_{ch} \rangle = A + B \ln W^2$.

Reaction	Intercept A	Slope B	χ^2/DF	
νD	0.05 ± 0.06	1.43 ± 0.02	1.34	This experiment
νn	-0.20 ± 0.07	1.42 ± 0.03	1.15	This experiment
νp	0.05 ± 0.08	1.42 ± 0.03	0.48	This experiment
νp	0.37 ± 0.02	1.33 ± 0.02		Ref. 2
νp		1.35 ± 0.15		Ref. 5

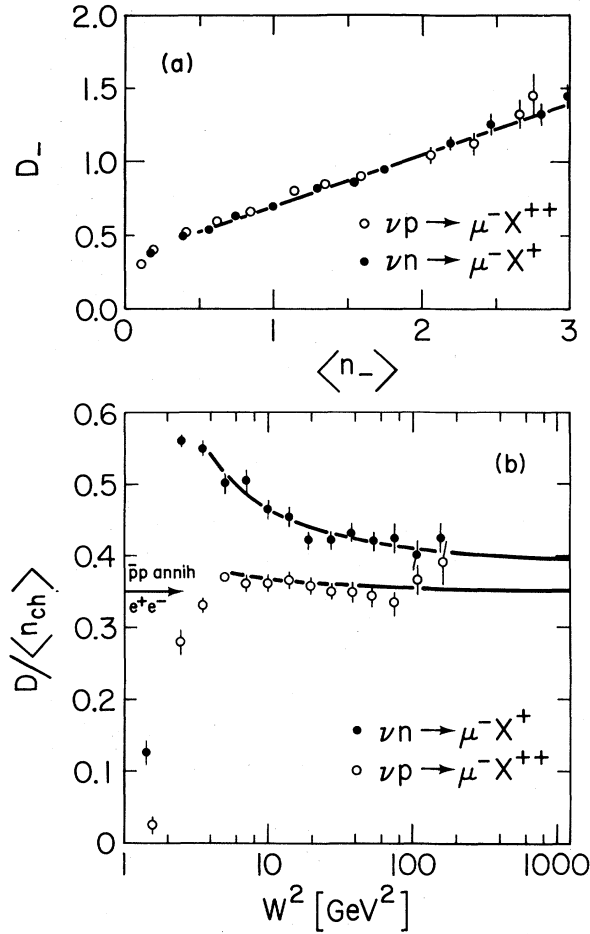


FIG. 5. (a) The dispersion $D_- = (\langle n_-^2 \rangle - \langle n_- \rangle^2)^{1/2}$ as a function of $\langle n_- \rangle$. The solid line is the linear fit to the νn data. (b) $D/\langle n_{ch} \rangle$ as a function of W^2 . The solid lines result from the relations $D = 0.32 + 0.36\langle n_{ch} \rangle$ for νn and $D = 0.10 + 0.34\langle n_{ch} \rangle$ for νp and from the relations between $\langle n_{ch} \rangle$ and W^2 listed in Table II.

main difference between the final states in νn and νp interactions lies, therefore, in the valence quark content of the diquark which is (ud) and (uu) , respectively, so that α may be identified with the difference $\langle n_- \rangle_{ud} - \langle n_- \rangle_{uu}$. In the final state, most of the negative particles are pions, whose quark content is $(d\bar{u})$. Thus, a π^- meson shares a valence quark only with a (ud) diquark. Therefore, one possible way to produce a positive value for α is for the (ud) diquark to break up and fragment independently. Alternatively α can be positive due to the increased probability for an excited baryon formed from a (ud) diquark to emit a negative meson as compared to its emission from a baryon formed from a (uu) diquark whose electric charge is greater by one unit. The measured values of α are between 0.15 and 0.35 (the corresponding values of $\langle n_{ch} \rangle_{\nu p} - \langle n_{ch} \rangle_{\nu n}$ are

between 0.7 and 0.3), depending on whether we use for the νp reaction data from our νD experiment or from the νH experiment of Ref. 2. These results mean that the fragmentation of the (ud) diquark gives rise to about 0.15–0.35 more negative hadrons per event, produced directly or via decay of an excited hadronic state, than does the fragmentation process of the (uu) diquark.

The difference between the mean multiplicity of negative particles produced on neutron and proton targets has been measured in high-energy hadron-nucleon interactions. There it is interpreted as a probability of the charge-exchange rate at the nucleonic vertex,

$$\begin{aligned} \alpha &= \sigma(n \rightarrow p\pi^- X) / \sigma(n \rightarrow \text{all}) \\ &= \sigma(p \rightarrow n\pi^+ X) / \sigma(p \rightarrow \text{all}) . \end{aligned}$$

The results for πN ,¹⁰ for pN (Ref. 11), and for photoproduction¹² are close to 0.3 at beam energies between 10 GeV and 20 GeV, which correspond to hadronic energies in this experiment, and increase to about 0.5 at energies above 100 GeV.¹³

C. DISPERSION AND KOBA-NIELSEN-OLESEN DISTRIBUTIONS

The dispersion $D_- = (\langle n_-^2 \rangle - \langle n_- \rangle^2)^{1/2}$ of the negative hadron multiplicity is plotted as a function of $\langle n_- \rangle$ in Fig. 5(a). Various values of $\langle n_- \rangle$ correspond to data grouped in the same W^2 intervals as in Table I and Figs. 3 and 4. The data exhibit a linear dependence

$$D_- = a + b\langle n_- \rangle . \quad (5)$$

The results of these fits for νn and νp interactions, shown in Table III, are very similar. They are also quite consistent with the values obtained for νp interactions observed in a νH experiment.²

The ratio $D/\langle n_{ch} \rangle$ as a function of W^2 is shown in Fig. 5(b). The curves in Fig. 5(b) result from the fits in Table III, which imply $D = 0.32 + 0.36\langle n_{ch} \rangle$ for νn and $D = 0.10 + 0.34\langle n_{ch} \rangle$ for νp and from relations between $\langle n_{ch} \rangle$ and W^2 listed in Table II. In the case of νp interactions the ratio $D/\langle n_{ch} \rangle$ is almost independent of energy for $W \geq 2$ GeV and is close to the value $b = 0.34$. For νn interactions $D/\langle n_{ch} \rangle$ approaches its asymptotic value from

TABLE III. Parameters of the linear fit to the dispersion distributions $D_- = a + b\langle n_- \rangle$. Note that $D = 2D_-$, $n_{ch} = 2n_- + 1$ for νn , and $n_{ch} = 2n_- + 2$ for νp .

Reaction	Intercept a	Slope b	χ^2/DF	
νn	0.34 ± 0.01	0.36 ± 0.01	0.92	This experiment
νp	0.39 ± 0.02	0.34 ± 0.02	0.41	This experiment
νp	0.36 ± 0.03	0.36 ± 0.03		Ref. 2

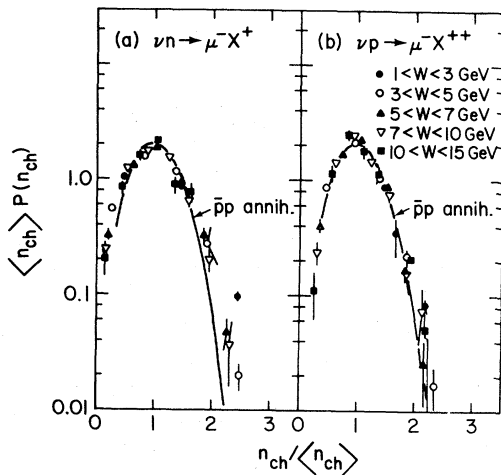


FIG. 6. KNO scaling distributions for (a) νn and for (b) νp interactions. The curve represents a fit to $\bar{p}p$ annihilation data, from Rushbrooke *et al.* (Ref. 16).

above, showing considerably more variation with W .

In Fig. 6 the dependence of $\langle n_{ch} \rangle P(n_{ch})$ on $n_{ch} / \langle n_{ch} \rangle$ is shown for five intervals of W , for the νn and νp samples. It is seen that in both cases the data approximately agree with Koba-Nielsen-Olesen (KNO) scaling,¹⁴ i.e., the points from differing W intervals lie approximately on a single curve. The agreement with KNO scaling is particularly good in the νp case, for which, as seen in Fig. 5(b), the ratio $D / \langle n_{ch} \rangle$ is close to its asymptotic value at relatively low energies. (Exact KNO scaling demands that the parameter a be equal to zero.) The behavior of the νp data on the KNO plot is similar to that found for the $\bar{p}p$ and e^+e^- annihilation data, whereas the distribution for the νn sample is slightly broader. We stress, however, that the dispersion data for the νn and νp samples more nearly coincide when studied in terms of n_- rather than in terms of the total charged-hadron multiplicity n_{ch} . This is not surprising since n_- is a closer measure of the number of pairs of mesons produced in the final state and is less dependent on the total hadronic charge.

D. DISCUSSION

The linear dependence of dispersion of the average multiplicity was first observed for hadron-hadron interactions¹⁵ and later confirmed in the case of lepton production,²⁻⁴ and in $\bar{p}p$ (Ref. 16) and e^+e^- annihilations.¹ The value of the slope $b=0.35$ is a common feature of both e^+e^- and lepton-nucleon collisions. It is the same, within errors, for $\bar{p}p$ annihilations, whereas the corresponding values reported in the literature for the πp and pp interactions is $b=0.57$. However, as predicted by Van Hove,¹⁷ and

as shown recently by Wroblewski,¹⁸ when the contribution of diffractive dissociation processes is subtracted from pp and πp cross sections the slope b of the function $D_-(\langle n_- \rangle)$ agrees with that found in other types of reactions.

The similarity of multiparticle distributions in high-energy hadron and lepton collisions has been stressed more recently by Goulianos and collaborators.^{19,20} For example, if one compares the probabilities for 1, 3, 5, and 7 charged particles that can be derived from our data listed in Table I(a) for νn collisions with the same probabilities given in Ref. 19 for the hadronic reactions $h^\pm + p \rightarrow X^\pm + p$, where $h = \pi^-$ or p , as functions of the available mass $M = W - M_n$, one finds almost identical results. However, the simple model proposed in Ref. 20 fails when applied to the νp data here and in Ref. 2. That model predicts much larger values for D_- from νp as compared to νn collisions for the same value of $\langle n_- \rangle$ whereas Fig. 5(a) shows that the D_- vs $\langle n_- \rangle$ curve is the same for νn and νp collisions.

The similarity of multiparticle distributions in high-energy hadron and lepton collisions suggests a universality of the hadron production mechanism. At the same time, it seems to be at odds with some theoretical models, where differences in the distributions of hadrons produced in hadron- and lepton-induced processes are predicted.

In the dual unitarization model^{21,22} the properties of particle production in various processes are related to the number of chains, or superclusters, which are formed as a result of $3\bar{3}$ color separation. In e^+e^- and IN interactions only one chain is produced (see Fig. 1). In hadron-hadron collisions two chains are predominantly formed while in $\bar{p}p$ annihilation one expects that three chains are predominantly formed. The multiplicity distributions in these latter cases are then described as convolutions of two or three single-chain distributions. The expected relation between the ratios of the dispersion to the mean multiplicity in $\bar{p}p$ annihilation, hN , IN , and e^+e^- is then²²

$$\left[\frac{D}{\langle n_{ch} \rangle} \right]_{\bar{p}p} : \left[\frac{D}{\langle n_{ch} \rangle} \right]_{hN} : \left[\frac{D}{\langle n_{ch} \rangle} \right]_{IN, e^+e^-} = 3^{-1/2} : 2^{-1/2} : 1 \quad (6)$$

Given the $D / \langle n \rangle \approx 0.35$ for the single-chain e^+e^- or IN collisions, the $\bar{p}p$ and hN values are much too high at presently available energies to fit this model. It has been shown,²³ however, that if the effect of the chain energy spread is taken into account the multiplicity dispersion data in pp collisions are described well by the dual model.

From a more fundamental point of view it has been pointed out²⁴ that the slope $b=0.57$ found for

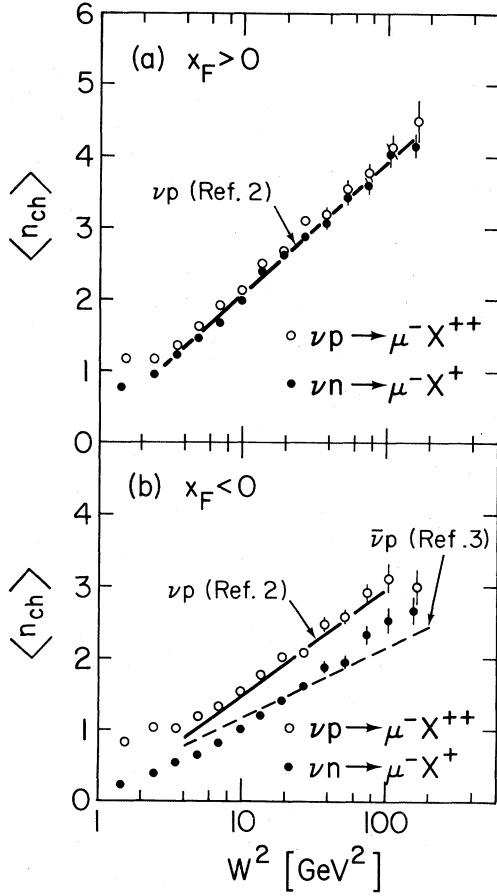


FIG. 7. Average charged-hadron multiplicity as a function of W^2 (a) in the forward ($x_F > 0$) and (b) backward ($x_F < 0$) hemispheres in the hadronic center of mass.

hp interactions (including diffractive events) is very close to the asymptotic value of $D_g/\langle n_g \rangle = \sqrt{1/3} = 0.577$ where D_g and $\langle n_g \rangle$ are the dispersion and multiplicity of gluon clusters of (mass)² = Q_0^2 , $\Lambda^2 \ll Q_0^2 \ll Q^2$, Λ being the scale parameter of QCD. The corresponding theoretical value for quarks is $D_q/\langle n_q \rangle = \sqrt{3/4} = 0.866$. Since in neutrino reactions one may expect that one quark jet gives a significant contribution to the total charged-particle multiplicity, that would suggest that $(D/\langle n_{ch} \rangle)_{\nu N} > (D/\langle n_{ch} \rangle)_{hN}$, again in disagreement with what we find. It should be pointed out that the predictions of the QCD calculus²⁴ involve partonic "final states," and that by applying them to the hadronic system one assumes that the final stage of hadron formation does not alter the results. Furthermore, more realistic theoretical calculations by Odorico²⁵ with the QCD calculus indicates that the asymptotic energy at which the prediction cited above for $D/\langle n_{ch} \rangle$ should hold is much higher than the region explored here.

IV. MULTIPLICITIES IN FORWARD AND BACKWARD HEMISPHERES

The multiplicities of charged particles in the forward ($x_F > 0$) and backward ($x_F < 0$) c.m. hemispheres can be studied separately. In Fig. 7 the mean multiplicities $\langle n_{ch} \rangle_{F,B}$ are shown as functions of W^2 for νn and νp interactions. As in the case of the overall multiplicities, each satisfies the relation $\langle n_{ch} \rangle_{F,B} = A + B \ln W^2$. The mean multiplicities of positive and negative particles, $\langle n_+ \rangle_{F,B}$ and $\langle n_- \rangle_{F,B}$, are shown in Fig. 8. According to the QPM, the dominant charged-current interaction makes a leading u quark for both n and p targets, with the remaining diquarks being (ud) and (uu), respectively. The subsequent processes of hadron formation are expected to be dependent on the quark or diquark flavor but not on the primary reaction from which they originate. The following observations are in agreement with this model:

(i) Within experimental uncertainties, the mean multiplicity of charged particles which follow the

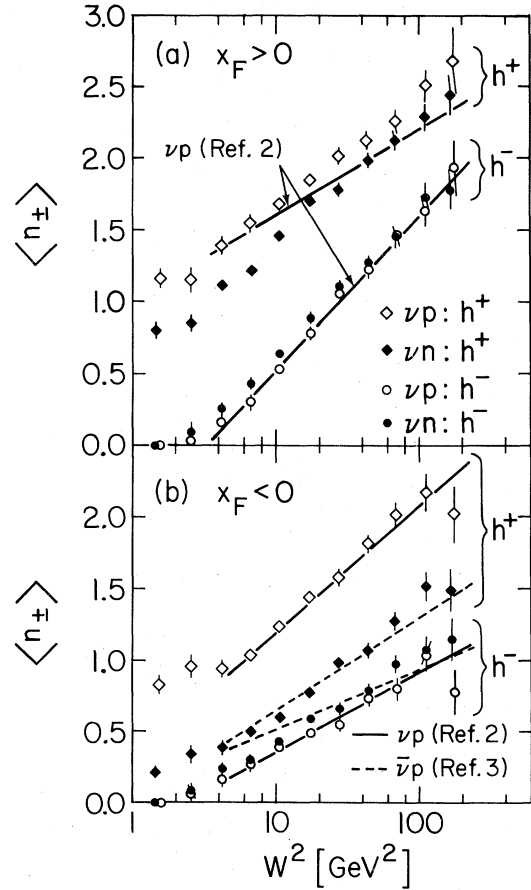


FIG. 8. Average charged-hadron multiplicity versus W^2 for positive and negative particles, separately. (a) $x_F > 0$; (b) $x_F < 0$.

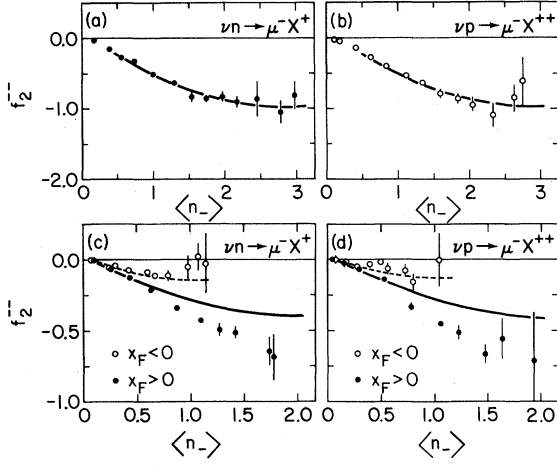


FIG. 9. The correlation parameter $f_2^{--} = \langle n_-(n_- - 1) \rangle - \langle n_- \rangle^2$ as a function of $\langle n_- \rangle$: (a) νn events, all x_F ; (b) νp events, all x_F ; (c) νn events, $x_F > 0$ and $x_F < 0$ separately; (d) νp events, $x_F > 0$ and $x_F < 0$, separately. The curves in (a) and (b) display the fits of Table III to D_- vs $\langle n_- \rangle$ and the relation $f_2^{--} = D_-^2 - \langle n_- \rangle$. The curves in (c) and (d) follow from the above fits and the assumption of the binomial distribution.

leading quark ($x_F > 0$) coincide for the νn and νp interactions. They agree with the results of the νH experiment of Ref. 2.

(ii) In the backward hemisphere, $\langle n_{ch} \rangle_B$ for νn is smaller than that for νp interactions. Instead, it agrees with $\langle n_{ch} \rangle_B$ for $\bar{\nu} p$ interactions³ where the spectator diquark is also (ud). Our νp data are similar to the results from the νH experiment,² although they lie slightly higher, presumably due to the re-scattering effect in deuterium.

More detailed information on particle production is provided by the study of higher moments of the multiplicities in the forward and backward hemispheres. We have determined the correlation parameter

$$f_2^{--} = \langle n_-(n_- - 1) \rangle - \langle n_- \rangle^2$$

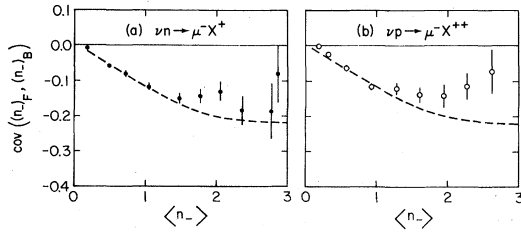


FIG. 10. Covariance $\text{cov}((n_-)_F, (n_-)_B)$ versus $\langle n_- \rangle$ in νn and νp scattering. The curves follow from the fits of Table III and from the assumption of the binomial distribution.

for all negative particles and the analogous parameters $(f_2^{--})_{F,B}$ for forward and backward negative particles. The results are presented in Fig. 9. The data on f_2^{--} as a function of $\langle n_- \rangle$ for all negative particles are shown in Figs. 9(a) and 9(b) for νn and νp , respectively. The curves follow from the linear fits of the dependence of D_- on $\langle n_- \rangle$ and from the equation $f_2^{--} = D_-^2 - \langle n_- \rangle$. The dependence of $(f_2^{--})_{F,B}$ on $\langle n_- \rangle_{F,B}$ is shown in Figs. 9(c) and 9(d). To calculate the curves we take the empirical dependence of f_2^{--} on $\langle n_- \rangle$ and we assume that particles are distributed randomly between the forward and backward hemispheres according to the binomial distribution

$$P(n, n_F) = P(n) \binom{n}{n_F} f^{n_F} b^{n_B}, \quad (7)$$

where $f + b = 1$ and $f/b = \langle n \rangle_F / \langle n \rangle_B$. The covariance²⁶ of $(n_-)_F$ and $(n_-)_B$,

$$\text{cov}((n_-)_F, (n_-)_B)$$

$$= \langle (n_-)_F (n_-)_B \rangle - \langle n_- \rangle_F \langle n_- \rangle_B,$$

which is related to the correlation parameters f_2^{--} by

$$2\text{cov}((n_-)_F, (n_-)_B) = f_2^{--} - (f_2^{--})_F - (f_2^{--})_B, \quad (8)$$

is shown in Fig. 10. While the binomial distribution of Eq. (7) qualitatively reproduces the trends in the data it does not yield a good fit. Another extreme assumption, namely, that forward and backward particles come from two independent, uncorrelated sources, implies the relation

$$f_2^{--} = (f_2^{--})_F + (f_2^{--})_B. \quad (9)$$

Equation (9) is not compatible with the experimental results shown in Figs. 9 and 10. The simple binomial distribution given in Eq. (7) gives a qualitative fit to the data but does not address the underlying physical interpretation of the nonvanishing forward-backward correlations. For example, simple energy conservation could play a role at our modest values of W . Nevertheless, this finding should serve as a warning against too literal a treatment of forward- and backward-going particles as fragmentation products of the current quark and the spectator diquark, respectively.

V. CONCLUSIONS

The mean multiplicities of charged hadrons produced in νn and νp interactions studied in deuterium are observed to increase logarithmically with W^2 in the range $2 \leq W \leq 15$ GeV. The slope of the increase, $B = 1.42$, is found to be equal for νn and νp

interactions. The mean multiplicity $\langle n_{\text{ch}} \rangle_{\nu p}$ measured in deuterium is larger by about 0.3 to 0.5 units than $\langle n_{\text{ch}} \rangle_{\nu p}$ measured in hydrogen possibly due to the rescattering in deuterium. The difference $\alpha = \langle n_- \rangle_{\nu n} - \langle n_- \rangle_{\nu p}$ is between 0.15 and 0.35, and can be interpreted as the excess of negative particles produced in (ud) diquark fragmentation over that in (uu) fragmentation. The values of α for deep-inelastic neutrino scattering are comparable to the value of 0.3 found in hadronic reactions and in photoproduction.

The dispersion of the multiplicity distribution shows a linear rise with mean multiplicity with a slope $b \simeq 0.35$ similar to that found in other neutrino experiments and in e^+e^- and $\bar{p}p$ annihilations. Although there are differences observed between the dependence of D on $\langle n_{\text{ch}} \rangle$ for n and p targets, the dependence of D_- on $\langle n_- \rangle$ is very similar for νn and νp interactions. In both cases KNO scaling is approximately satisfied. In our energy region, neither the dependence of $\langle n_{\text{ch}} \rangle$ on W , nor the comparison of $D/\langle n_{\text{ch}} \rangle$ for lepton-nucleon and hadron-nucleon interactions shows effects predicted by asymptotic QCD.

Data on mean multiplicity for forward and back-

ward hemispheres in the hadronic center-of-mass system are consistent with QPM. The mean multiplicities are similar for νn and νp at $x_F > 0$, where the leading quark is a u quark in both cases. Differences are seen in the backward hemisphere, where the leading systems are (ud) and (uu) , respectively. On the other hand, the νn data resemble the $\bar{\nu}p$ data, for which the spectator diquark is also a (ud) system.

The correlation parameter f_2^- for the forward and backward hemispheres has also been measured, and found in qualitative agreement with the simple assumption of a binomial distribution of particles between the two hemispheres.

ACKNOWLEDGMENTS

We thank the members of the Accelerator Division and Neutrino Department at Fermilab for their essential work. We are particularly indebted to the scanning and measuring staffs at our respective laboratories who helped to extract the data from the film. This research is supported in part by the U. S. Department of Energy and the National Science Foundation.

*On leave from the University of Warsaw, Warsaw, Poland.

†Present address: Bell Telephone Laboratories, Naperville, Illinois 60540.

‡Present address: Notre Dame University, Notre Dame, Indiana 46556.

¹PLUTO Collaboration, Ch. Berger *et al.*, Phys. Lett. **78B**, 176 (1978); **95B**, 313 (1980); ADONE, C. Bacci *et al.*, *ibid.* **86B**, 234 (1979); SLAC, J. L. Siegrist, Ph.D. thesis, Report No. SLAC-225 UC-34d, 1980 (unpublished); TASSO Collaboration, W. Brandelik *et al.*, Phys. Lett. **89B**, 418 (1980); JADE Collaboration, W. Bartel *et al.*, *ibid.* **88B**, 171 (1979).

²P. Allen *et al.*, Nucl. Phys. **B181**, 385 (1981).

³S. Barlag *et al.*, Z. Phys. C **11**, 283 (1982).

⁴M. Derrick *et al.*, Phys. Rev. D **25**, 624 (1982).

⁵J. Bell *et al.*, Phys. Rev. D **19**, 1 (1979).

⁶H. G. Heilmann, Bonn Internal Report No. WA21-int 1, 1978 (unpublished).

⁷R. D. Field and R. P. Feynman, Phys. Rev. D **15**, 2590 (1977); Nucl. Phys. **B136**, 1 (1978).

⁸J. Hanlon *et al.*, Phys. Lett. **45**, 1817 (1980).

⁹R. P. Feynman, Phys. Rev. Lett. **23**, 1415 (1969).

¹⁰H. Abramowicz *et al.*, Z. Phys. C **7**, 199 (1981).

¹¹D. Hochman *et al.*, Nucl. Phys. **B89**, 383 (1975); V. Blobel *et al.*, *ibid.* **B80**, 189 (1974).

¹²Y. Eisenberg *et al.*, Nucl. Phys. **B104**, 61 (1976).

¹³Y. Eisenberg *et al.*, Phys. Lett. **60B**, 305 (1976); J. E.

Lys *et al.*, Phys. Rev. D **16**, 3127 (1977).

¹⁴Z. Koba, H. B. Nielsen, and P. Olesen, Nucl. Phys. **B40**, 317 (1972).

¹⁵A. Wroblewski, in *Proceedings of the Third International Colloquium on Multiparticle Reactions, Zakopane, Poland, 1972*, edited by O. Czyzweski and L. Michejda (Nuclear Energy Information Center of the Polish Government Commissioner, Warsaw, 1972), p. 140; Acta Phys. Pol. **B4**, 857 (1973).

¹⁶R. Stenbacka *et al.*, Nuovo Cimento **51A**, 63 (1979); P. D. Gall, Ph.D. thesis, DESY Report No. F1 76/02, 1976 (unpublished); F. T. Das *et al.*, Phys. Lett. **51B**, 505 (1974); L. N. Abesalashvili *et al.*, *ibid.* **52B**, 236 (1974); M. A. Jabiol *et al.*, Nucl. Phys. **B127**, 365 (1977); R. M. Robertson *et al.*, Phys. Rev. D **21**, 3054 (1980); J. Rushbrooke *et al.*, Phys. Lett. **59B**, 303 (1975).

¹⁷L. Van Hove, Phys. Lett. **43B**, 64 (1973).

¹⁸A. Wroblewski, in *Multiparticle Dynamics 1981*, proceedings of the XII International Symposium, Notre Dame, Indiana, edited by W. D. Shephard and V. P. Kenney (World Scientific, Singapore, 1982).

¹⁹R. L. Cool *et al.*, Phys. Rev. Lett. **48**, 1451 (1982).

²⁰K. Goulianos *et al.*, Phys. Rev. Lett. **48**, 1454 (1982).

²¹X. Artru and G. Menessier, Nucl. Phys. **B70**, 93 (1974); G. Veneziano, *ibid.* **B74**, 365 (1974); **B117**, 519 (1976); J. Dias de Deus, *ibid.* **B123**, 240 (1977); A. Rossi and G. Veneziano, *ibid.* **B125**, 507 (1977); G. F. Chew and

- A. Rosenzweig, Phys. Rep. 410, 263 (1978); A. Capella, Phys. Lett. 81B, 68 (1979).
- ²²J. Dias de Deus, Phys. Lett. 100B, 177 (1981).
- ²³K. Fialkowski and A. Kotanski, Phys. Lett. 107B, 137 (1981).
- ²⁴K. Konishi, A. Ukawa, and G. Veneziano, Phys. Lett. 78B, 243 (1978); Nucl. Phys. B157, 45 (1979).
- ²⁵R. Odorico, Nucl. Phys. B172, 157 (1980); Phys. Lett. 102B, 341 (1981).
- ²⁶S. Brandt, *Statistical and Computational Methods in Data Analysis* (North-Holland, Amsterdam, 1970).